20th Australasian Fluid Mechanics Conference
Perth, Australia
5-8 December 2016

# Approximate Solutions to the Linearized Navier-Stokes Equations for Incompressible Channel Flow

**A. Leonard**

Graduate Aerospace Laboratories
California Institute of Technology
Pasadena, California 91125, USA

### Abstract

The linearized Navier-Stokes equations for incompressible channel flow are considered in which the flow is homogeneous in two directions. We study the initial-value problem for $\upsilon$ and $\omega_y$, where $y$ is the coordinate normal to the wall. After a Laplace transform in time and a double Fourier transform in space we use the WKB approximation on the resulting system of ODE's in $y$ to construct analytically the Green's function for such solutions for the inviscid case in terms of the Bessel functions $J_1$ and $Y_1$, their modified counterparts, and the Airy functions $Ai$ and $Bi$.

### Introduction

In a number of recent investigations of wall-bounded flows, solutions to the linearized Navier-Stokes equations have played a major role. Such examples are the study of the origin and role of very large scale structures in the dynamics of turbulent pipe flow (McKeon and Sharma [4]) and the development and application of low-complexity models to investigate the statistics of wall-bounded turbulent flows (Zare *et. al* [5]). In both cases the authors had to undertake a significant computational effort to compute the resolvent of the Orr-Sommerfeld/Squire operator.

In this paper, we find, semi-analytically, solutions to the inviscid linearized equations for channel flow. After a Laplace transform in time and a double Fourier transform in space we use the WKB approximation (see, e.g., Bender and Orszag [1]) on the resulting system of ODE's in $y$ to construct analytically the Green's function for such solutions in terms of the Bessel functions $J_1$ and $Y_1$, their modified counterparts, and the Airy functions $Ai$ and $Bi$. In this approach the critical layers or the $y$ locations where $U(y) = \omega/k_x$ require special attention, when they exist, as well as the locations of the turning points where $d^2U/dy^2 = (k_x^2+k_z^2)(\omega/k_x - U(y))$, when they exist. This analysis then gives analytically the response of the linear system to an arbitrary forcing function, facilitating the investigation of many aspects of turbulent flows. Not considered in this paper are viscous corrections to the inviscid solutions that are required at the walls at the critical layers. Use of the WKB approximation for this application has along history. See, e.g., Drazin and Reid [2].

### Linearized Navier-Stokes Equations

Consider flow in a plane channel with walls at $y = \pm\delta$ and periodic boundary conditions in the $x$ and $z$ directions. In the following we will be working in Fourier space in the $x$ and $z$ directions. The steady mean flow and vorticity are give as

$$\begin{aligned} \mathbf{U} &= (U(y), 0, 0) \\ \Omega &= (0, 0, -dU(y)/dy) \end{aligned} \quad (1)$$

We assume the flow is symmetric, i.e., $U(-y) = U(y)$ and that $dU/dy \geq 0$ for $|y| \leq \delta$. The linearized Navier-Stokes equations for $\upsilon$ and $\omega_y$, Laplace transformed in time, are then

$$(U(y)-c)\left(\frac{d^2\upsilon}{dy^2} - k_\perp^2\upsilon\right) - U''(y)\upsilon = \frac{-i\nu}{k_x}\left(\frac{d^2}{dy^2} - k_\perp^2\right)^2\upsilon - \frac{i}{k_x}\upsilon_0 \quad (2)$$

$$(U(y)-c)\omega_y + \frac{k_z}{k_x}U'(y)\upsilon = \frac{-i\nu}{k_x}\left(\frac{d^2}{dy^2} - k_\perp^2\right)\omega_y - \frac{i}{k_x}\omega_{y0}, \quad (3)$$

where $k_\perp^2 = k_x^2 + k_z^2, c = \omega/k_x$, and $s = -i\omega$ is the Laplace transform variable.The initial functions of $\upsilon$ and $\omega_y$ in time are $\upsilon_0$ and $\omega_{y0}$, respectively. The other velocity components, $u$ and $w$, are then recoverable from the incompressiblity constraint and the expression for $\omega_y$ in terms of derivatives of $u$ and $w$.

### Analysis of the Inviscid Equations

We consider first the homogeneous inviscid equation for $\upsilon$, i.e. (2) with $\nu$ and $\upsilon_0 = 0$.

$$\frac{d^2\upsilon}{dy^2} - \left(\frac{U''(y)}{U(y)-c} + k_\perp^2\right)\upsilon = 0. \quad (4)$$

We assume (4) is amenable to a WKB solution

so that $\upsilon(y)$ is given approximately as

$$\upsilon(y) = \chi^{-1/4}(y)\exp\left(\pm i\int^y \sqrt{\chi(y')}dy'\right), \quad (5)$$

where

$$\chi(y) = -\frac{U''(y)}{U(y)-c} - k_\perp^2 \quad (6)$$

Thus (6) should give a good approximation for $\upsilon(y)$ as long as $|\chi(y)| >> |\partial\sqrt{\chi(y)}/\partial y|$. Note, therefore, the approximation will likely fail at turning points of $\chi(y)$, i.e., $y$ locations where $\chi(y) = 0$. In our case so there are two potential turning points: $\pm y_c$ where $U(\pm y_c) = c$ (assuming $c$ is real) and potentially two more at $\pm y^*$ where $\frac{U''(\pm y^*)}{U(\pm y^*)-c} + k_\perp^2 = 0$. In the former case the approximate equation for $\upsilon$ near $y = y_c$ is

$$(y-y_c)\upsilon'' - \frac{U''(y_c)}{U'(y_c)}\upsilon = 0, \quad (7)$$

with solutions

$$\begin{aligned} \upsilon = \quad & A \quad (y-y_c)^{1/2}J_1 \quad 2\sqrt{-\frac{U''(y_c)}{U'(y_c)}(y-y_c)}\Bigg) + \quad (8) \\ & B \quad (y-y_c)^{1/2}Y_1 \quad 2\sqrt{-\frac{U''(y_c)}{U'(y_c)}(y-y_c)}\Bigg), \end{aligned}$$

where $J_1$ and $Y_1$ are Bessel functions. On the other hand, (5 -6) give the solutions

$$\upsilon = \left[-\frac{U''(y)}{U(y)-c} - k_\perp^2\right]^{-1/4} \exp\left(\pm i \int_y^{y_c} \sqrt{-\frac{U''(y')}{U(y')-c} - k_\perp^2}\, dy'\right) \tag{9}$$

away from $y = y_c$. Next, following Langer [3], we note that both (8) and (9) are satisfied with the choice $\upsilon = \upsilon(y; y_c)$ given by

$$\begin{aligned} \upsilon(y; \pm y_c) &= A_\pm \frac{[\pm h_+(y, \pm y_c)]^{1/2}}{\chi(y)^{1/4}} J_1(\pm h_+(y, \pm y_c)) \\ &+ B_\pm \frac{[\pm h_+(y, \pm y_c)]^{1/2}}{\chi(y)^{1/4}} Y_1(\pm h_+(y, \pm y_c)), \end{aligned} \tag{10}$$

where

$$\chi(y) = -\frac{U''(y)}{U(y)-c} - k_\perp^2, \tag{11}$$

and

$$h_\pm(y_1, y_2) = \int_{y_2}^{y_1} \sqrt{\pm\chi(y')}\, dy', \tag{12}$$

and we have anticipated the solution $\upsilon(y; -y_c)$ for $y$ in the neighborhood of $-y_c$. One can verify that (9) is compatible with (10) by using the facts that

$$\begin{aligned} J_\nu(z) &\to \sqrt{\frac{2}{\pi z}} \cos(z - \frac{1}{2}\nu\pi - \frac{1}{4}\pi) \\ Y_\nu(z) &\to \sqrt{\frac{2}{\pi z}} \sin(z - \frac{1}{2}\nu\pi - \frac{1}{4}\pi) \end{aligned} \tag{13}$$

as $|z| \to \infty$ with $|\arg(z)| < \pi$.

Similarly, near $y = y^*$ (see the discussion after Eq.(6)), the ODE for $\upsilon$ reduces to

$$\upsilon'' + \alpha(y - y^*)\upsilon = 0, \tag{14}$$

where $\alpha = \frac{d}{dy}\left(\frac{-U''(y)}{U(y)-c}\right)|_{y=y^*}$,with solutions

$$\begin{aligned} \upsilon = &\ C \quad Ai(-\alpha^{1/3}(y - y^*)) \\ + &\ D \quad Bi(-\alpha^{1/3}(y - y^*)), \end{aligned} \tag{15}$$

where $Ai$ and $Bi$ are Airy functions. Away from $y = y^*$ the solutions are given by (9) with $y_c$ replaced by $y^*$. Again, the near and away solutions for both $\pm y^*$ are satisfied by

$$\begin{aligned} \upsilon(y; \pm y^*) = &\ C_\pm \quad \frac{[\pm h_+(y, \pm y^*)]^{1/6}}{[\chi(y)^{1/4}]} Ai(\pm h_+(y, \pm y^*)) \\ + &\ D_\pm \quad \frac{[\pm h_+(y, \pm y^*)]^{1/6}}{[\chi(y)^{1/4}]} Bi(\pm h_+(y, \pm y^*)). \end{aligned} \tag{16}$$

## Patching Solutions Together

We assume $\omega$ is real for the moment. Then if $0 < c = \omega/k_x < U(0) = U_{max}$ then there exists a $y_c$ satisfying $U(\pm y_c) = c$. Similarly, if $-U''(0)/(U(0) - c) < k_\perp^2$ then there exists a $y^*$ such that $-U''(\pm y^*)/(U(\pm y^*) - c) = k_\perp^2$.

Consider the case where $\pm y_c$ exist but $\pm y^*$ do not. Then $\upsilon(y, y_c)$ will be a valid solution for $0 \le y \le \delta$ while $\upsilon(y, -y_c)$ will be valid for $-\delta \le y \le 0$, both given by (10). Enforcing $\upsilon(0, +y_c) = \upsilon(0, -y_c)$ and $\upsilon'(0, +y_c) = \upsilon'(0, -y_c)$, we find that

$$\begin{aligned} A_+ &= \frac{\pi}{2}[\Theta(Y_0(\Theta)J_1(\Theta) + Y_1(\Theta)J_0(\Theta) - Y_1(\Theta)J_1(\Theta)]A_- \\ &+\pi\left[\Theta Y_0(\Theta)Y_1(\Theta) - \frac{1}{2}Y_1(\Theta)^2\right]B_- \\ B_+ &= -\pi\left[\Theta J_0(\Theta)J_1(\Theta) - \frac{1}{2}J_1(\Theta)^2\right]A_- \\ &-\frac{\pi}{2}[\Theta(Y_0(\Theta)J_1(\Theta) + Y_1(\Theta)J_0(\Theta) - Y_1(\Theta)J_1(\Theta)]B_-, \end{aligned} \tag{17}$$

where $\Theta = \int_0^{y_c} \sqrt{\chi(y')}\, dy'$. If we assume that the asymptotic formulas for the Bessel functions (16) hold in the vicinity of $y = 0$ , we find readily that $\upsilon(y; y_c)$ and $\upsilon(y; -y_c)$ match exactly if

$$\begin{aligned} A_- &= -A_+ \sin 2\Theta + B_+ \cos 2\Theta \\ B_- &= A_+ \cos 2\Theta + B_+ \sin 2\Theta. \end{aligned} \tag{18}$$

The case in which $\pm y^*$ exist but $\pm y_c$ do not proceeds in an analogous manner. In this case patching at $y = 0$ will involve the functions defined by (16) and their derivatives.

Finally, when both $\pm y^*$ and $\pm y_c$ exist, patching must be done at three locations: between between $-y_c$ and $-y^*$ , between $-y^*$ and $y^*$, and between $y^*$ and $y_c$. Matching the functions and their first derivatives at a specific location gives the required connection.

## $\chi$ Negative

The solutions (10) are appropriate when $\chi$ is positive yielding oscillatory functions. They are still valid when $\chi$ is negative but not necessarily convenient. In this case, we can express (10) in terms of modified Bessel functions. For example, for $y > y_c$ and the choice $\sqrt{\chi} = -i\sqrt{-\chi}$ (10) for $\upsilon(y; y_c)$ becomes

$$\begin{aligned} \upsilon(y; y_c) = &- \frac{[h_-(y_c, y)]^{1/2}}{[-\chi(y)]^{1/4}}(A_+ + iB_+)I_1(h_-(y_c, y)) \\ &- \frac{[h_-(y_c, y)]^{1/2}}{[-\chi(y)]^{1/4}}\frac{2}{\pi}B_+ K_1(h_-(y_c, y)). \end{aligned} \tag{19}$$

## Green's Function for $\upsilon(y)$

The Green's function $G(y, y_o)$ for (4) satisfies

$$\frac{d^2G}{dy^2} - \left(\frac{U''(y)}{U(y)-c} + k_\perp^2\right)G = \delta(y - y_o), \tag{20}$$

with boundary conditions $G(\pm\delta, y_o) = 0$. Consider the case in which $\pm y_c$ exist but $\pm y^*$ do not and suppose $y_o > y_c$. Then, for $y > y_o$, a component of $G$ is given by

$$G_+(y,y_o) = -\frac{[h_-(y_c,y)]^{1/2}}{[-\chi(y)]^{1/4}} K_1(\Psi) I_1(h_-(y_c,y)) + \frac{[h_-(y_c,y)]^{1/2}}{[-\chi(y)]^{1/4}} I_1(\Psi) K_1(h_-(y_c,y)), \quad (21)$$

satisfying $G_+(\delta) = 0$, where $\Psi = \int_{y_c}^{\delta} \sqrt{-\chi(y')}dy'$. At the same time, we find similarly that another component of $G$ for $-\delta \leq y \leq 0$ is given by

$$G_-(y,y_o) = -\frac{[h_-(y,-y_c)]^{1/2}}{[-\chi(y)]^{1/4}} K_1(\Psi) I_1(h_-(y,-y_c)) + \frac{[h_-(y,-y_c)]^{1/2}}{[-\chi(y)]^{1/4}} I_1(\Psi) K_1(h_-(y,-y_c)), \quad (22)$$

satisfying $G_-(-\delta, y_o) = 0$.

Next we need to continue the component (22) all the way to the interval $y_c < y < \delta$ where $y_o$ is located. Again using the choice $\sqrt{\chi} = -i\sqrt{-\chi}$ we find that (22) may be expressed as

$$G_-(y,y_o) = \frac{[h_+(-y_c,y)]^{1/2}}{[\chi(y)]^{1/4}} (K_1(\Psi) + \frac{i\pi}{2} I_1(\Psi)) J_1(h_+(-y_c,y)) - \frac{[h_+(-y_c,y)]^{1/2}}{[\chi(y)]^{1/4}} \frac{\pi}{2} I_1(\Psi) Y_1(h_+(-y_c,y)), \quad (23)$$

suitable for the interval $-y_c \leq y \leq 0$. Now using the connection or patching formulas (17), we determine $G$ as

$$G_-(y,y_o) = A_+ \frac{[h_+(y,y_c)]^{1/2}}{\chi(y)^{1/4}} J_1(h_+(y,y_c)) + B_+ \frac{[h_+(y,y_c)]^{1/2}}{\chi(y)^{1/4}} Y_1(h_+(y,y_c)), \quad (24)$$

in the interval $0 \leq y \leq y_c$ with

$$\begin{aligned} A_+ &= -K_1(\Psi)\sin\Theta_{JY} - \frac{\pi}{2} I_1(\Psi)(\cos\Theta_Y + i\sin\Theta_{JY}) \\ B_+ &= K_1(\Psi)\cos\Theta_J + \frac{\pi i}{2} I_1(\Psi)(\cos\Theta_J + i\sin\Theta_{JY}), \end{aligned} \quad (25)$$

where

$$\begin{aligned} \cos\Theta_J &= -\pi\left[\Theta J_0(\Theta) J_1(\Theta) - \frac{1}{2} J_1(\Theta)^2\right] \\ \cos\Theta_Y &= \pi\left[\Theta Y_0(\Theta) Y_1(\Theta) - \frac{1}{2} Y_1(\Theta)^2\right] \\ \sin\Theta_{JY} &= -\frac{\pi}{2}\left[\Theta(Y_0(\Theta) J_1(\Theta) + Y_1(\Theta) J_0(\Theta)) - Y_1(\Theta) J_1(\Theta)\right]. \end{aligned} \quad (26)$$

Each of the $\Theta_J, \Theta_Y$, and $\Theta_{JY} \to 2\Theta$ as each of them $\to \infty$. Finally, we use (19) again to rewrite (24) in terms of modified Bessel functions:

$$G_-(y,y_o) = \frac{[h_-(y_c,y)]^{1/2}}{[-\chi(y)]^{1/4}} \left[p_- I_1(h_-(y_c,y)) + q_- K_1(h_-(y_c,y))\right], \quad (27)$$

to give $G_-(y,y_o)$ in the interval $y_c \leq y \leq y_o$. where

$$\begin{aligned} p_- &= -iK_1(\Psi)(\cos\Theta_J + i\sin\Theta_{JY}) \\ &\quad + \frac{\pi}{2} I_1(\Psi)(\cos\Theta_Y + \cos\Theta_J + 2i\sin\Theta_{JY}) \\ q_- &= -\frac{2}{\pi} K_1(\Psi)\cos\Theta_J - iI_1(\Psi)(\cos\Theta_Y + i\sin\Theta_{JY}). \end{aligned} \quad (28)$$

Using (24) we see that the analogous factors for $G_+$ are

$$\begin{aligned} p_+ &= -K_1(\Psi) \\ q_+ &= I_1(\Psi) \end{aligned} \quad (29)$$

To construct the Green's function we note that $G$ defined by

$$\begin{aligned} G(y,y_o) &= \alpha G_-(y) G_+(y_o) \quad (y < y_o) \\ &= \alpha G_-(y_o) G_+(y) \quad (y > y_o) \end{aligned} \quad (30)$$

is continuous at $y = y_o$ and satisfies $G(\pm\delta, y_o) = 0$. By using the condition

$$\frac{\partial G}{\partial y}|_{y-y_o=0^+} - \frac{\partial G}{\partial y}|_{y-y_o=0^-} = 1 \quad (31)$$

we find that $\alpha$ is given by

$$\alpha = \frac{1}{2(p_+ q_- - p_- q_+)}. \quad (32)$$

A similar analysis will produce the Green's function for the case in which both $\pm y_c$ and $\pm y*$ exist. In addition, it is rather straightforward to find the solution to (3) for $\omega_y(y)$ once $\upsilon$ has been determined.

### Example: Plane Poiseuille Flow

In this section we apply our analysis to the case of plane Poiseuille flow: $U(y) = U_o(1 - y^2/\delta^2)$. We choose to nondimensionalize by setting $U_o = \delta = 1$ so that $\chi(y) = 2/(1 - c - y^2) - k_\perp^2$. Therefore $y_c = \sqrt{1-c}$, if $0 \leq c \leq 1$, and $y^*$ will exist if $k_\perp^2(1-c) \geq 2$ and, if so, $y^* = \sqrt{1 - c - 2/k_\perp^2}$.

Figs. 1-5 show results for the coefficient of the Green's function, $\alpha$, for small positive and negative $c$. (See Eqs. (30) and (32)). Note that the coefficient has significant amplitude only in a narrow strip of the $(c, k_\perp)$ plane. And from Figure 3 note that there is a one-dimensional family of solutions for $c < 0$ where $\alpha = \infty$ corresponding to homogeneous solutions to the inviscid equation (3) with $c$ real. For $c > 0$ homogeneous solutions also exist but for $c$ complex as implied by Figs. 4 and 5.

### Conclusions

Semi-analytical solutions to the inviscid linearized equations for channel flow are determined. After a Laplace transform in time and a double Fourier transform in space the WKB approximation is used on the resulting system of ODE's in $y$ to construct the Green's function for such solutions in terms of the Bessel functions $J_1$ and $Y_1$, their modified counterparts, and the Airy functions $Ai$ and $Bi$. Here the critical layers or the $y$ locations where $U(y) = \omega/k_x$ require special attention, when they exist, as well as the locations of the turning points where $d^2U/dy^2 = (k_x^2 + k_z^2)(\omega/k_x - U(y))$, when they exist. This analysis then gives the response of the linear system to an arbitrary

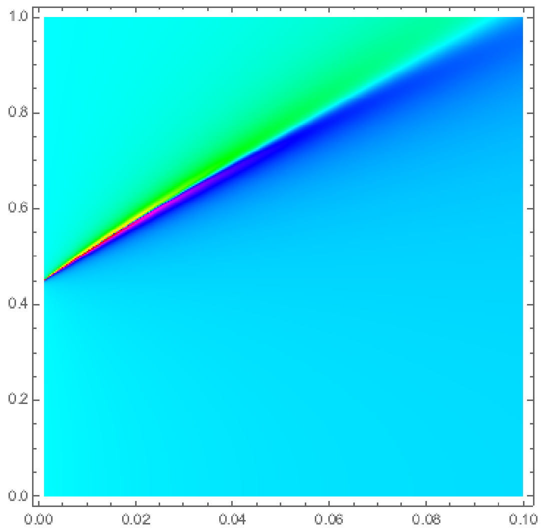


Figure 1: Real part of $\alpha$ in the $(c, k_\perp)$ plane for $c$ positive. Red, amplitude $\approx +10$; Yellow, amplitude $\approx -10$.

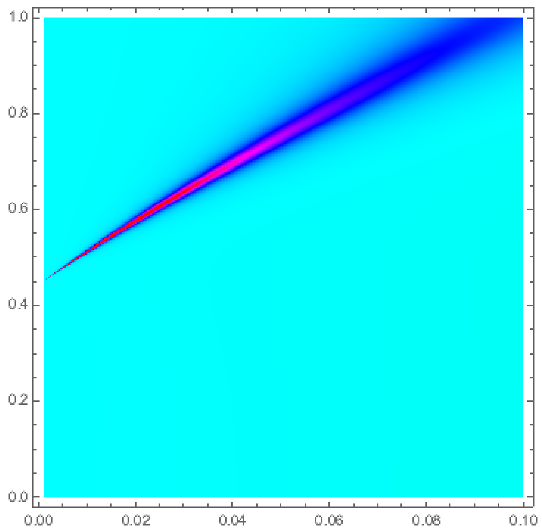


Figure 2: Imaginary part of $\alpha$ in the $(c, k_\perp)$ plane for $c$ positive. Red, amplitude $\approx +10$.

forcing function, facilitating the investigation of many aspects of turbulent flows. Viscous corrections to the inviscid solutions will be required at the walls and at the critical layers. Application to the case of plane Poiseuille flow has revealed a narrow strip of high-amplitude solutions for the Green's function in the $(c, k_\perp)$ plane including a one-dimensional family of homogeneous solutions to the inviscid equations with $c$ real for $c < 0$ and $c$ complex for $c > 0$.

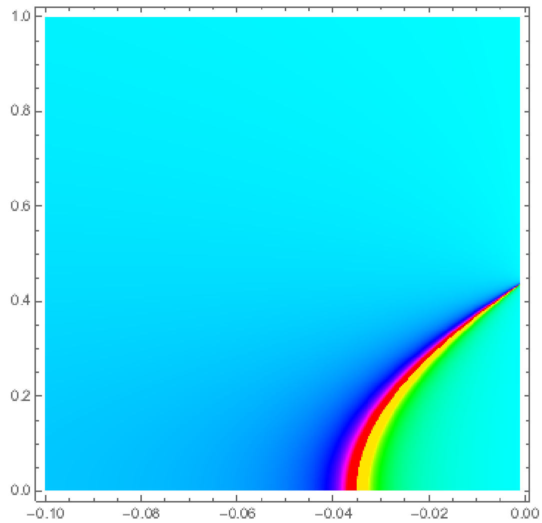


Figure 3: $\alpha$ in the $(c, k_\perp)$ plane for $c$ negative. Red, amplitude $\approx +10$; Yellow, amplitude $\approx -10$. Higher amplitudes are clipped for clarity. Along the line separating red and yellow $\alpha = \infty$.

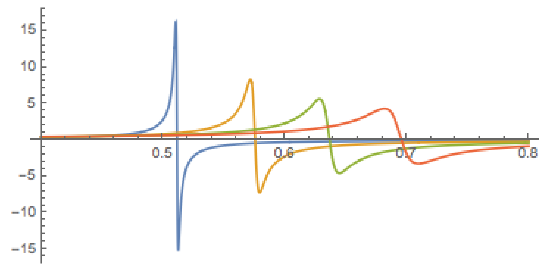


Figure 4: Real part of $\alpha$ versus $k_\perp$. Blue, $c = 0.01$; Orange, $c = 0.02$; Green, $c = 0.03$; Red, $c = 0.04$.

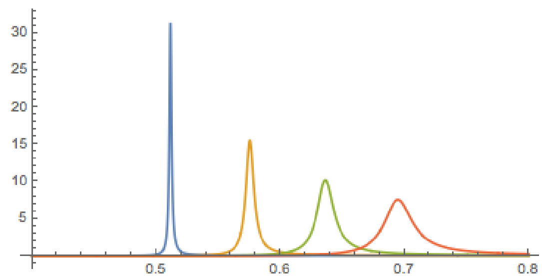


Figure 5: Imaginary part of $\alpha$ versus $k_\perp$. Blue, $c = 0.01$; Orange, $c = 0.02$; Green, $c = 0.03$; Red, $c = 0.04$.

## References


[1] Bender, C. M. and Orszag, S. A., *Advanced Mathematical Methods for Scientists and Engineers*, McGraw-Hill, 1978.

[2] Drazin, P. G. and Reid, W. H., *Hydrodynamic Stability*, Cambridge University Press, 1981.

[3] Langer, R. E., On the Connection Formulas and the Solutions of the Wave Equation, *Phys. Rev.* **51**, 669-676, 1937 See also Langer, R. E. *Bull. Am. Math. Soc.* **37**, 397, 1935.

[4] McKeon, B. J. and Sharma, A. S., A critical-layer framework for turbulent pipe flow, *J. Fluid Mech.* **658**, 336-382, 2010.

[5] Zare, A., Jovanović, M. R. and Georgiou, T. T. , Color of turbulence, *J. Fluid Mech.*, 2016 (submitted).